

Interference of high-order harmonics generated from molecules at different alignment angles

Meiyan Qin^{1,2}, Xiaosong Zhu^{1,2}, Yang Li^{1,2}, Qingbin Zhang^{1,2}, Pengfei Lan^{1,2}*, and Peixiang Lu^{1,2}†

¹ *School of Physics and Wuhan National Laboratory for Optoelectronics,
Huazhong University of Science and Technology, Wuhan 430074, China*

² *Key Laboratory of Fundamental Physical Quantities Measurement of MOE, Wuhan 430074, China*

(Dated: July 6, 2021)

We theoretically investigate the interference effect of high-order harmonics generated from molecules at different alignment angles. It is shown that the interference of the harmonic emissions from molecules aligned at different angles can significantly modulate the spectra and result in the anomalous harmonic cutoffs observed in a recent experiment [*Nature Phys.* 7, 822 (2011)]. The shift of the spectral minimum position with decreasing the degree of alignment is also explained by the interference effect of the harmonic emissions.

PACS numbers: 32.80.Rm, 42.65.Ky

I. INTRODUCTION

High-order harmonic generation (HHG) from molecules has attracted a great deal of attention, due to the amazing application in probing the molecular structure and electron dynamics with attosecond and Ångström resolutions[1–8]. A rich set of new physical phenomena such as the spectral minimum have been experimentally observed [9–15]. In these experiments, the target molecules were impulsively excited into a rotational wave packet by a moderately intense pump pulse to achieve the field-free alignment [16, 17]. And then a more intense probe pulse at a certain time delay with respect to the pump pulse was focused into these partially aligned molecules to generate the high-order harmonics. The distribution of the angle between the molecular axis and the polarization of the probe pulse varies with the time delay. Therefore, to simulate these pump-probe experiments, the alignment distribution of the molecules at a certain time delay should be taken into account. In previous theoretical works, two alternative methods were adopted to take into account the partial alignment of molecules. In Refs.[12, 13, 18], a noncoherent superposition of the harmonic intensities convolved with the angular distribution is adopted to explain the experimental observations. While in Refs.

[4, 10, 11], a coherent sum of the harmonic emissions is employed to simulate the HHG from partially aligned molecules.

The spectral minimum is one of the most important phenomena observed in the molecular HHG. Both the interference of the harmonic emissions from different nuclei in a molecule and the interference of the harmonic emissions from multiple channels can modulate the harmonic spectrum and induce a spectral minimum [19, 20]. With a detailed analysis of these minima, the information about the molecular structure and electron dynamics can be extracted [15, 21]. It is shown that the harmonic spectrum is also modulated due to the effect of the partial alignment of molecules [9, 22, 23], which is inevitable in the actual experiment. Whereas how the interference of the harmonic emissions from molecules at different alignment angles affects the harmonic spectrum is seldom investigated. Knowing this interference effect may provide a route to quasi-phase-matching. Moreover, it helps us correctly extract the information about the molecular structure and electron dynamics.

In this paper, we investigate the interference effect of the harmonic emissions from molecules at different alignment angles. By comparing the harmonic spectra obtained with the coherent and noncoherent superpositions of the harmonic emissions with those measured in experiment, it is confirmed that the harmonic emissions from molecules at different alignment angles superpose coherently. We perform a detailed analysis of the interference effect at different time delays and with different

*Corresponding author: pengfeilan@mail.hust.edu.cn

†Corresponding author: lupeixiang@mail.hust.edu.cn

degrees of alignment. It is shown that the anomalous harmonic cutoff phenomenon observed in a recent experiment [10] and the shift of the spectral minimum position with decreasing the degree of alignment can be explained by the interference effect of the harmonic emissions from molecules at different alignment angles.

II. THEORETICAL MODEL

To calculate the HHG spectrum for a fixed alignment, we use the strong field approximation (SFA) model for molecules [24, 25]. Within the single active electron (SAE) approximation, the time-dependent dipole velocity is given by

$$\begin{aligned} \mathbf{v}_{dip}(t; \theta) = & i \int_{-\infty}^t dt' \left[\frac{\pi}{\zeta + i(t-t')/2} \right]^{\frac{3}{2}} \exp[-iS_{st}(t', t)] \\ & \times \mathbf{F}(t') \cdot \mathbf{d}_{ion} [\mathbf{p}_{st}(t', t) + \mathbf{A}(t'); \theta] \\ & \times \mathbf{v}_{rec}^* [\mathbf{p}_{st}(t', t) + \mathbf{A}(t); \theta] + c.c.. \end{aligned} \quad (1)$$

In this equation, ζ is a positive constant. t' and t correspond to the ionization and recombination time of the electron, respectively. θ is the alignment angle between the molecular axis and the polarization of the probe pulse. $\mathbf{F}(t)$ refers to the electric field of the probe pulse, and $\mathbf{A}(t)$ is its associated vector potential. \mathbf{p}_{st} and S_{st} are the stationary momentum and the quasi-classical action, which are given by

$$\mathbf{p}_{st}(t', t) = -\frac{1}{t-t'} \int_{t'}^t \mathbf{A}(t'') dt'' \quad (2)$$

and

$$S_{st}(t', t) = \int_{t'}^t \left(\frac{[\mathbf{p}_{st} + \mathbf{A}(t'')]^2}{2} + I_p \right) dt'' \quad (3)$$

with I_p being the ionization energy of the state that the electron is ionized from. Then the complex amplitude of the high-order harmonics with a frequency ω_n is given by

$$\tilde{\mathbf{E}}(\omega_n, \theta) = \int e^{i\omega_n t} \frac{d}{dt} \mathbf{v}_{dip}(t; \theta) dt. \quad (4)$$

When the coherent superposition of the harmonic emissions is employed to take into account the partial alignment of the molecules, the spectrum at the delay τ with respect to the pump pulse is given by

$$S(\omega_n; \tau) = \left| \int E(\omega_n, \theta) \exp[iP(\omega_n, \theta)] \rho(\theta; \tau) d\theta \right|^2. \quad (5)$$

When the noncoherent superposition is adopted, the spectrum at the delay τ is given by

$$S(\omega_n; \tau) = \int I(\omega_n, \theta) \rho(\theta; \tau) d\theta. \quad (6)$$

In the two formulae, $E(\omega_n, \theta) = |\tilde{\mathbf{E}}(\omega_n, \theta)|$, $P(\omega_n, \theta) = \arg(\tilde{\mathbf{E}}(\omega_n, \theta))$, and $I(\omega_n, \theta) = |\tilde{\mathbf{E}}(\omega_n, \theta)|^2$ are the amplitude, phase, and intensity of the high-order harmonics generated from the molecule aligned at θ . $\rho(\theta; \tau)$ is the weighted angular distribution and is given by

$$\begin{aligned} \rho(\theta; \tau) = & \sin \theta (1/Z) \sum_{J_i} Q(J_i) \\ & \times \sum_{M_i=-J_i}^{J_i} \int |\Psi^{J_i M_i}(\theta, \phi; \tau)|^2 d\phi. \end{aligned} \quad (7)$$

Here $Q(J_i) = \exp(-BJ_i(J_i+1)/(k_B T))$ is the Boltzmann distribution function of the initial field-free state $|J_i, M_i\rangle$ at temperature T , $Z = \sum_{J=0}^{J_{max}} (2J+1)Q(J)$ is the partition function, k_B and B are the Boltzmann constant and the rotational constant of the molecule, respectively. $\Psi^{J_i M_i}(\theta, \phi; \tau)$ is the time-dependent rotational wave packet excited from the initial state $|J_i, M_i\rangle$ by the pump pulse, and is obtained by solving the time dependent Schrödinger equation (TDSE) within the rigid-rotor approximation [16, 17]

$$i \frac{\partial \Psi(\theta, \phi; \tau)}{\partial t} = [B\mathbf{J}^2 - \frac{E_p(\tau)^2}{2} (\alpha_{\parallel} \cos^2 \theta + \alpha_{\perp} \sin^2 \theta)] \Psi(\theta, \phi; \tau). \quad (8)$$

In this equation, α_{\parallel} and α_{\perp} are the anisotropic polarizabilities in parallel and perpendicular directions with respect to the molecular axis, respectively. The degree of alignment is characterized by the alignment parameter $\langle \cos^2 \theta \rangle$, and is given by

$$\begin{aligned} \langle \cos^2 \theta \rangle (\tau) = & (1/Z) \sum_{J_i} Q(J_i) \\ & \times \sum_{M_i=-J_i}^{J_i} \langle \Psi^{J_i M_i}(\theta, \phi; \tau) | \cos^2 \theta | \Psi^{J_i M_i}(\theta, \phi; \tau) \rangle. \end{aligned} \quad (9)$$

III. RESULT AND DISCUSSION

We choose the CO₂ molecule as an example for investigating the interference effect of the harmonic emissions from molecules at different alignment angles. In our simulation, a 100 fs (FWHM) 800 nm linearly polarized pump pulse with an intensity of 4.0×10^{13} W/cm² is used to non-adiabatically align the CO₂ molecule and

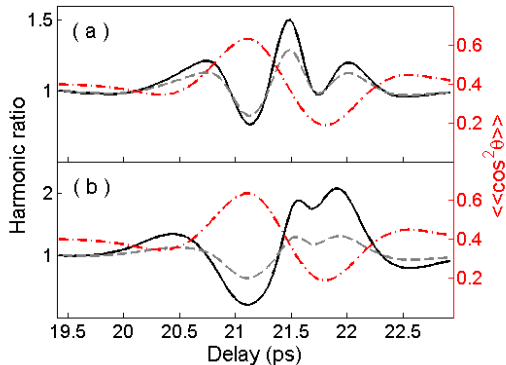


FIG. 1: (Color online) Ratio between harmonic signal generated in aligned and unaligned CO_2 molecules for the harmonics at photon energies 35.72 eV (panel a) and 51.25 eV (panel b). The results obtained with the coherent and noncoherent superposition methods are presented by solid black and dashed grey lines respectively. The time evolution of the alignment parameter $\langle \cos^2 \theta \rangle (\tau)$ is also displayed by the dash-dotted red line.

the initial rotational temperature is taken to be 40 K. For the CO_2 molecule, only even- J states are populated in the ground state due to the spin statistics [26]. Hence, rotational states $|J, M\rangle$ with $J = 0, 2, 4, \dots, 24$ are included in our calculation. Then a delayed probe pulse with the polarization parallel to that of the pump pulse is used to generate high-order harmonics. The wavelength, pulse duration, and intensity of the probe pulse are 1450 nm, 18 fs (FWHM), and 1.2×10^{14} W/cm², respectively. These parameters of the pump and probe pulses are the same as those used in the recent pump-probe experiment [10]. In that work, the interference of harmonic emissions from multiple channels is shown to be negligible when a few-cycle mid-IR (1450 nm) probe pulse is used. Therefore the HHG can be well described within the SAE approximation.

In our simulation, both the coherent and noncoherent superpositions of the harmonic emissions are adopted to include the partial alignment effect. We first calculate the time evolution of the high-order harmonics at a fixed photon energy. The time delay around the first half revival ($\tau = 21.1$ ps) is considered. In Fig. 1, the ratios between harmonic signals generated from aligned and unaligned CO_2 molecules are presented for the high harmonics at photon energies 35.72 eV (panel a) and 51.25 eV (panel b). The solid black and dashed grey lines show the results obtained with Eq. (5) and Eq. (6), respectively. The time evolution of the alignment parameter

$\langle \cos^2 \theta \rangle (\tau)$ is also displayed by the dash-dotted red line. As shown in Fig. 1, both the harmonic ratios obtained by the coherent and noncoherent superposition present inverted modulation with respect to the molecular alignment. These inverted modulations of the harmonic ratios at 35.72 eV and 51.25 eV are experimentally observed in Ref. [9] and Ref. [13] respectively, and are explained by the two-center interference effect. In Ref. [13], it is demonstrated that with the noncoherent superposition method the inverted modulation of the harmonic ratio can be satisfactorily reproduced. Whereas our results show that not only the noncoherent but also the coherent superpositions of the harmonic emissions can predict the inverted modulations of the harmonic ratios at 35.72 eV and 51.25 eV.

We also calculate the whole spectrum as a function of the time delay. The results are presented in Fig. 2. As shown in Fig. 2(a), the harmonic spectra obtained by employing the coherent superposition agree well with the observations of the recent pump-probe experiment [10]. In detail, obvious spectral minima are observed at the delays around 21.1 ps. Furthermore, the spectral cutoffs at the delays around 21.1 ps and 21.81 ps appear at 84.7 eV. While in the harmonic spectra at other delays the cutoffs are observed at much lower photon energies, which can not be explained by the cutoff-law

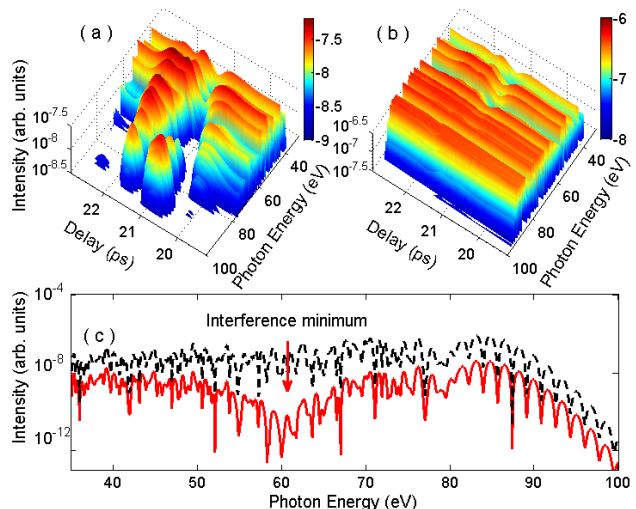


FIG. 2: (Color online) Harmonic spectra as a function of the time delay obtained with coherent (panel a) and noncoherent (panel b) superposition method. (c) Harmonic spectra at the time delay 21.1 ps for the coherent (solid red line) and noncoherent (dashed black line) superposition cases.

$I_p + 3.17U_p$. This anomalous cutoff phenomenon is described as the cutoff recession in Ref. [10]. As for the noncoherent superposition case shown in Fig. 2(b), however, both the interference minima and the cutoff recession phenomenon are missing. For clarity, the harmonic spectra at the delay time 21.1 ps are presented in Fig. 2(c) for the coherent (the solid red line) and noncoherent (the dashed black line) superposition cases. As indicated by the red arrow, an obvious minimum occurs only in the spectrum obtained by employing the coherent superposition. Moreover, the spectral minimum position (60.3 eV) is the same as that measured in Ref. [10]. Therefore, only the coherent superposition of the harmonic emissions from molecules aligned at different angles can fully describe the HHG from partially aligned molecules. Although some features of the HHG can be reproduced by the noncoherent superposition of the harmonic emissions as shown in Fig. 1 and also shown in Ref. [13], the more accurate description of the HHG from partially aligned molecules is the coherent superposition. Our results confirm that the harmonic emissions from molecules at different alignment angles superpose coherently.

To provide insights into the anomalous harmonic cutoff phenomenon observed in experiment [10], we perform an analysis of the angular-dependent amplitudes and phases of the harmonics near the cutoff in perfect alignment case. In Fig. 3(a), the amplitude ($E(\omega_n, \theta)$) and phase ($P(\omega_n, \theta)$) of the harmonic emission at photon energy 77.5 eV, where the harmonic cutoff recession occurs, are presented. As shown in Fig. 3(a), the harmonic emissions near the cutoff exhibit two-center interference minima around 50° , which is accompanied by a phase jump of π . Thus, the harmonic emissions are divided by the 50° angle into two parts that have π phase difference. For the first part $\theta < 50^\circ$, the corresponding harmonic phases are around 0.5π , while for the second part $\theta > 50^\circ$, the phases are around -0.5π . As a result, when coherently superposing the harmonic emissions at different alignment angles, the interference of the harmonic emissions will modulate the observed spectra, depending on the corresponding angular distribution. In Figs. 3(b-d), the polar plot of $\rho(\theta; \tau)$ at three typical delays 21.1 ps, 21.81 ps, and 22.85 ps are presented, respectively. At the first half revival delay 21.1 ps, the CO_2 molecules are mostly aligned along the laser polarization direction ($\theta = 0^\circ$). The corresponding weighted angular distribution maximizes at 24° , as shown in Fig. 3(b). Thus at delays

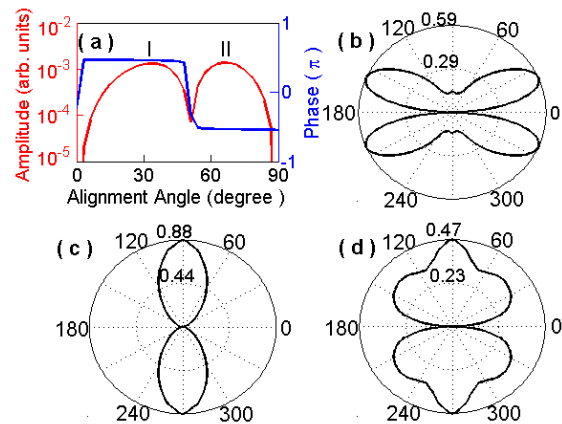


FIG. 3: (Color online) (a) The angular-dependent amplitude (solid red line) and phase (solid blue line) of the harmonic emission at photon energy 77.5 eV in perfect alignment case. (b-d) The polar plots of the angular distributions $\rho(\theta; \tau)$ at the delays 21.1 ps (b), 21.81 ps (c) and 22.85 ps (d).

around 21.1 ps the harmonics near the cutoff are determined by the constructive interference of the harmonic emissions from molecules aligned at the angles $\theta < 50^\circ$. At delays around 21.81 ps, the CO_2 molecules are mostly aligned perpendicular to the laser polarization ($\theta = 90^\circ$). The corresponding weighted angular distribution maximizes at 90° , as shown in Fig. 3(c). Thus the harmonics near the cutoff are determined by the constructive interference of the harmonic emissions from molecules at the alignment angles $\theta > 50^\circ$. Correspondingly, the spectral cutoffs at delays around 21.1 ps and 21.81 ps appear at the photon energy 84.7 eV, which agrees with the cutoff-law $I_p + 3.17U_p$. While at other delays (for example at 22.85 ps as shown in Fig. 3(d)), the molecular alignment is quasi-random. The emissions at the alignment angles below and above 50° contribute almost equally to the high-order harmonics near the cutoff, i.e. the contributions of the two parts with π phase difference are comparable. Hence the harmonics near the cutoff are significantly suppressed due to the destructive interference. As a result, the harmonic spectra present cutoff recessions with respect to those around 21.1 ps and 21.81 ps. From the above analysis, one can see that the anomalous cutoff phenomenon results from the interference of the emissions from molecules aligned at different angles.

When the destructive interference of the harmonic emissions from molecules at different alignment angles occurs in the cutoff region, the cutoff recession appears. While if the destructive interference occurs at lower pho-

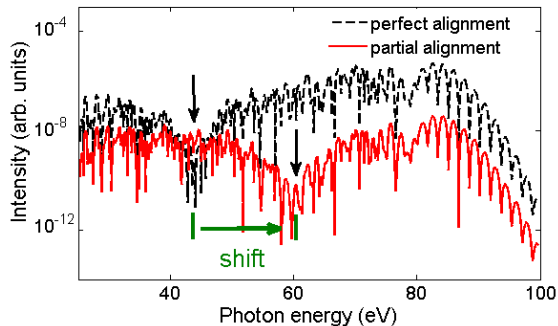


FIG. 4: (Color online) The harmonic spectra generated from CO₂ molecules in perfect alignment at 24° (dashed black line) and in partial alignment at the delay 21.1 ps (solid red line).

ton energies (i.e., in the plateau region), a well-defined spectral minimum will be observed. For high-order harmonics at a low photon energy, the associated phase jump by $\sim \pi$ occurs at a small angle. Accordingly, the destructive interference between the harmonic emissions at different alignment angles appears at the delays (such as 21.1 ps), when the molecules are mostly aligned at small angles. As a result, well-defined spectral minima are observed at the delays around 21.1 ps, as presented in Fig. 2(a). In the following, we compare the minimum positions in the harmonic spectra generated from perfectly and partially aligned molecules. As shown in Fig. 3(b), the angular distribution at the delay 21.1 ps for the CO₂ molecules maximizes at 24°. Therefore, we use the harmonic spectrum from CO₂ molecules perfectly aligned at 24° as a reference. In Fig. 4, both the harmonic spectra generated from perfectly (dashed black line) and partially (solid red line) aligned molecules are presented. The horizontal axis represents the photon energy. As shown in Fig. 4, the interference minimum in the harmonic spectrum for the perfect alignment is observed at photon energy 43.8 eV, which agrees with the two-center interference model with the dispersion relation $n\hbar\omega = E_k + I_p$. While after taking into account the partial alignment of molecules, the minimum appears at a higher energy 60.3 eV. Hence, the interference of the harmonic emissions at different alignment angles significantly shifts the spectral minimum position.

Next, we investigate how the spectral minimum position is affected by the interference of the harmonic emissions from molecules at different alignment angles. In Fig. 5(a), the harmonic spectra at the first half revival are presented for $\langle \cos^2\theta \rangle$ as 0.57 (dash-dotted red line), 0.50 (dashed green line), and 0.43 (solid blue

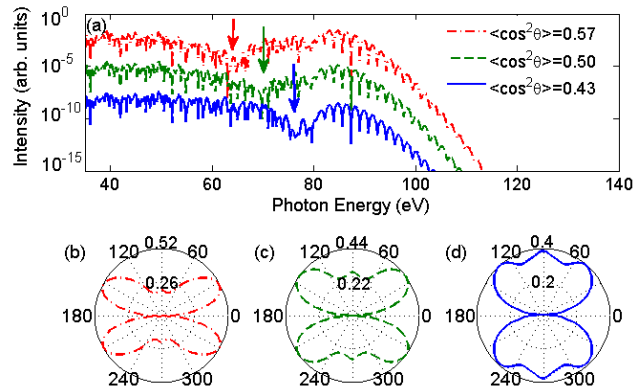


FIG. 5: (Color online) (a) Harmonic spectra at the first half revival with $\langle \cos^2\theta \rangle$ as 0.57 (dash-dotted red line), 0.50 (dashed green line) and 0.43 (solid blue line). The harmonic spectra for $\langle \cos^2\theta \rangle$ as 0.57 and 0.50 are vertically shifted for clarity. (b-d) Polar plot of the corresponding weighted alignment distributions for $\langle \cos^2\theta \rangle$ as 0.57 (b), 0.50 (c) and 0.43 (d).

line). These three degrees of alignment are achieved by using the pump pulse with intensities 3.0×10^{13} W/cm², 2.0×10^{13} W/cm², and 1.0×10^{13} W/cm², respectively. As shown in Fig. 5(a), the minimum position shifts to higher photon energies when the degree of alignment decreases. The same phenomenon has been observed experimentally in Ref. [23]. To explain this phenomenon, the corresponding weighted alignment distributions are presented in Figs. 5(b-d) for these three degrees of alignment. As shown in Figs. 5(b-d), the angle where the weighted alignment distribution maximizes shifts to a large angle with decreasing the degree of alignment. Simultaneously, the contributions from large alignment angles gradually increase. As discussed in Fig. (3), the critical angle, where a phase jump occurs, divides the harmonics into two parts with a π phase difference. When the contributions from the two parts are comparable, the most significant destructive interference of the harmonic emissions from different alignments (i.e. a spectral minimum) will occur at the corresponding high-order harmonics. In the case with a low value of $\langle \cos^2\theta \rangle$, the critical angle that associates with a phase jump of π and divides the harmonic emissions into two comparable parts shifts to a large angle. According to the two-center interference model, the high-order harmonics with the phase jump at a larger angle has a higher photon energy. As a result,

the spectral minimum will shift to a higher energy with the degree of alignment decreasing.

IV. CONCLUSION

In conclusion, we investigate the interference effect of the harmonic emissions from molecules at different alignment angles. By comparing the harmonic spectra obtained in our simulation with those measured in experiment, it is confirmed that the harmonic emissions from molecules at different alignment angles superpose coherently. We perform a detailed analysis of the interference effect of the high-order harmonics from partially aligned molecules at different time delays and with different degrees of alignment. It is shown that the interference of the

harmonic emissions from molecules aligned at different angles can significantly modulate the harmonic spectrum and result in the cutoff recession phenomenon observed in a recent experiment [10]. The shift of the spectral minimum position with decreasing the degree of alignment is also explained by the interference effect of the harmonic emissions.

V. ACKNOWLEDGMENTS

This work was supported by the NNSF of China under Grants No. 11234004 and 60925021, the 973 Program of China under Grant No. 2011CB808103 and the Doctoral fund of Ministry of Education of China under Grant No. 20100142110047.

-
- [1] M. Lein, N. Hay, R. Velotta, J. P. Marangos, and P. L. Knight, *Phys. Rev. Lett.* **88**, 183903 (2002).
- [2] J. Itatani, J. Levesque, D. Zeidler, H. Niikura, H. Pépin, J. C. Kieffer, P. B. Corkum and D. M. Villeneuve, *Nature* **432**, 867 (2004).
- [3] P. Lan *et al.*, *Phys. Rev. A* **76**, 011402(R) (2007); W. Hong, *et al.* *J. Opt. Soc. Am. B* **25** 1684-1689 (2008); J. Luo *et al.* *J. Phys. B* **46** 145602 (2013).
- [4] R. Torres, N. Kajumba, J. G. Underwood, J. S. Robinson, S. Baker, J. W. G. Tisch, R. deNalda, W. A. Bryan, R. Velotta, C. Altucci, I. C. E. Turcu, and J. P. Marangos, *Phys. Rev. Lett.* **98**, 203007 (2007).
- [5] H. J. Wörner, J. B. Bertrand, D. V. Kartashov, P. B. Corkum and D. M. Villeneuve, *Nature* **466**, 604 (2010).
- [6] X. Zhu, Q. Zhang, W. Hong, P. Lan, and P. Lu, *Opt. Express* **19**, 436 (2010).
- [7] S. Haessler, J. Caillat and P. Salières, *J. Phys. B: At. Mol. Opt. Phys.* **44**, 203001 (2011).
- [8] Y. Zhou *et al.* *Phys. Rev. Lett.* **109**, 053004 (2012); Q. Liao *et al.* *New J. Phys.* **14** 013001 (2012); C. Huang *et al.* *Opt. Express* **21** 11382 (2013).
- [9] T. Kanai, S. Minemoto and H. Sakai, *Nature* **435**, 470 (2005).
- [10] C. Vozzi, M. Negro, F. Calegari, G. Sansone, M. Nisoli, S. De Silvestri and S. Stagira, *Nature Phys.* **7**, 822 (2011).
- [11] X. Zhou, R. Lock, W. Li, N. Wagner, M. M. Murnane, and H. C. Kapteyn, *Phys. Rev. Lett.* **100**, 073902 (2008).
- [12] P. Liu, P. Yu, Z. Zeng, H. Xiong, X. Ge, R. Li, and Z. Xu, *Phys. Rev. A* **78**, 015802 (2008).
- [13] C. Vozzi, F. Calegari, E. Benedetti, J. P. Caumes, G. Sansone, S. Stagira, and M. Nisoli, R. Torres, E. Heesel, N. Kajumba, and J. P. Marangos, C. Altucci, R. Velotta, *Phys. Rev. Lett.* **95**, 153902 (2005).
- [14] X. Zhou, R. Lock, N. Wagner, W. Li, H. C. Kapteyn, and M. M. Murnane, *Phys. Rev. Lett.* **102**, 073902 (2009).
- [15] R. M. Lock, S. Ramakrishna, X. Zhou, H. C. Kapteyn, M. M. Murnane, and T. Seideman, *Phys. Rev. Lett.* **108**, 133901 (2012).
- [16] J. Ortigoso and M. Rodriguez, M. Gupta and B. Friedrich, *J. Chem. Phys.* **110**, 3870 (1999).
- [17] T. Seideman, *Phys. Rev. Lett.* **83**, 4971 (1999).
- [18] A. T. Le, X. M. Tong, and C. D. Lin, *Phys. Rev. A* **73**, 041402(R) (2006).
- [19] M. Lein, N. Hay, R. Velotta, J. P. Marangos, and P. L. Knight, *Phys. Rev. A* **66**, 023805 (2002).
- [20] O. Smirnova, S. Patchkovskii, Y. Mairesse, N. Dudovich, D. Villeneuve, P. Corkum, and M. Yu. Ivanov, *Phys. Rev. Lett.* **102**, 063601 (2009).
- [21] O. Smirnova, Y. Mairesse, S. Patchkovskii, N. Dudovich, D. Villeneuve, P. Corkum, and M. Yu. Ivanov, *Nature* **460**, 972 (2009).
- [22] C. Jin, A. T. Le, and C. D. Lin, *Phys. Rev. A* **83**, 053409 (2011).
- [23] A. Rupenyan, P. M. Kraus, J. Schneider, and H. J. Wörner, *Phys. Rev. A* **87**, 031401(R) (2013).
- [24] M. Lewenstein, Ph. Balcou, M. Yu. Ivanov, A. L’Huillier, and P. B. Corkum, *Phys. Rev. A* **49**, 2117 (1994).
- [25] M. Qin, X. Zhu, Q. Zhang, and P. Lu, *Opt. Letters* **37**, 5208 (2012).
- [26] K. Miyazaki, M. Kaku, G. Miyaji, A. Abdurrouf, and F. H. M. Faisal, *Phys. Rev. Lett.* **95**, 243903 (2005).